PREPARATION, CHARACTERIZATION AND TESTING OF CR/ALSBA-15 ETHYLENE POLYMERIZATION CATALYSTS

G. Calleja, J. Aguado, A.Carrero* and J. Moreno

Department of Chemical and Environmental Technology. ESCET.

Rey Juan Carlos University, 28933, Móstoles (Madrid), Spain.

Published on:

Applied Catalysis A: General 316 (2007) 22-31

doi:10.1016/j.apcata.2006.09.012

* To whom the correspondence should be addressed. Phone: 34-91-4888088. Fax: 34-91-4887068.

e-mail: alicia.carrero@urjc.es

Abstract

Ethylene polymerization catalysts have been prepared by grafting chromium (III) acetylacetonate onto SBA-15 (Si/Al = ∞, 156, 86 and 30) mesoporous materials. Aluminium incorporation favoured chromium anchorage onto SBA-15 surface as chromate and dichromate. The reduction temperature, determined by hydrogen TPR, decreased with the Si/Al ratio. Attachment of Cr species onto AlSBA-15 surface resulted from the interaction of hydroxyl groups with the acetylacetonate ligands through H-bonds, while a ligand exchange reaction may occur over siliceous SBA-15.

The polymerization catalyst corresponding to AlSBA-15 (Si/Al = 30) support is almost four times more active than a conventional Cr/SiO_2 Phillips catalyst. However, very poor polymerization activity was obtained with chromium supported on aluminium free SBA-15 material. Polymers obtained with all catalysts showed melting temperatures, bulk densities and high load melt indexes indicating the formation of linear high-density polyethylene.

Keywords: Mesoporous, SBA-15, AlSBA-15, chromium, ethylene polymerization.

1. Introduction

One of the most commercially important examples of supported transition metal catalysts are the Phillips catalysts (Cr/SiO_2) for ethylene polymerization, discovered in the early 1950's by J.P. Hogan and R.L. Banks working for the Phillips Company [1]. Since then, this catalytic system has been developed to become responsible for the production of more than one third of all polyethylene sold worldwide. Conventional preparation methods for Phillips catalysts involve the impregnation of an inorganic support (silica, alumina, aluminophosphates, etc) with an inorganic or organo-metallic chromium compound, followed by high temperature calcination (500-1000 ºC) to produce Cr(VI) active species [2-4]. Nowadays, it is well known that activity of Phillips catalysts is very sensitive to the composition and physicochemical properties of the solid supports, which play an important role on the resulting properties of the polyethylene produced [2, 3, 5].

Although silica is the usual support for the preparation of active polymerization catalysts, Al_2O_3, TiO_2, SiO_2-Al_2O_3 and ZrO_2 have also been used as solid carriers. Studies based on chromium supported over these materials indicated that different chromium species can be anchored to the support surface depending on its nature. For example, Weckhuysen et al. [6] found that monochromate species are the dominant in chromium supported on alumina, magnesium oxide and titanium dioxide, however dichromate species predominated in chromium supported on silica. Pullukat et al. [7] reported that the polymerization activity of chromium supported on alumina was one order of magnitude lower than chromium supported on silica systems. Furthermore, chromium supported on alumina catalysts produced polyethylene with higher molecular weight [7, 8].

Textural properties of the support have also a significant influence on Phillips catalysts behaviour. So, chromium supported on high pore volume silica presents a high catalytic activity

and therefore produces a low molecular weight polyethylene with high melt index. On the contrary, small pore size silica gives less active catalysts leading to high molecular weight polyethylene [2, 9].

The above commented results evidence that both, support pore size and pore volume, play an important role in the Phillips catalysts performance. In this way, recently discovered mesostructured materials are very attractive supports for the development of novel chromium supported catalysts for ethylene polymerization [10, 11]. One of them is SBA-15 mesostructured silica, which was synthesized by Zhao et al. in 1998 using amphiphillic triblock copolymers to direct the organization of silica species under strong acid conditions [12, 13]. This material is a well ordered hexagonal mesoporous silica structure with uniform pore size, which can be modified from 50 to 300 Å by using different triblock copolymers or by adding organic molecules as cosolvents [12, 13]. The preparation of aluminium-containing SBA-15 materials is difficult by the strong acid conditions required in the synthesis. Under such conditions, metals will exist only in the cationic form and therefore aluminium species cannot be introduced in the mesostructure via condensation process with silicon species [14]. However, Yue et al. have reported a successful direct synthesis of aluminium-containing SBA-15 materials by using a triblock copolymer as template at a pH value of 1.5 [15].

Here, we report the synthesis and characterization of several aluminium-containing SBA-15 materials with different Si/Al ratios and their behaviour in ethylene polymerization after chromium incorporation by grafting. These mesostructured catalysts have been compared with a chromium-containing amorphous catalyst prepared through grafting of chromium species onto a commercial silica (EP-10, Crosfield).

2. Experimental

2.1. Catalysts preparation.

Siliceous SBA-15 material was synthesized according to the procedure described by Zhao et al. [12] using Pluronic 123 triblock copolymer (EO_{20}-PO_{70}-EO_{20}; Aldrich) as template. In a typical synthesis: 4 g of Pluronic 123 was dissolved under stirring in 125 mg of 1.9 M HCl at room temperature. The solution was heated up to 40 ºC before adding tetraethylorthosilicate (TEOS; Aldrich). The resultant solution was stirred for 20 h at 40 ºC, followed by aging at 110 ºC for 24 h under static conditions. The solid product was recovered by filtration and dried at room temperature overnight. The template was removed from the as-made mesoporous material by calcination at 550 ºC for 5 h (heating rate = 1.8 ºC min^{-1}). **This calcined support was denoted as SBA-15.**

AlSBA-15 materials were prepared according to the direct synthesis procedure reported by Yue et al [15]. In a typical synthesis: 8.6 g of tetraethylorthosilicate (TEOS; Aldrich) and a calculated amount of aluminum isopropoxide (AIP; Aldrich), to obtain a given Si/Al ratio **(30, 60 and 90)**, were added to 10 ml of aqueous HCl at pH 1.5. This mixture was stirred for 4 h at room temperature and then added to a second solution containing 4 g of Pluronic 123 in 150 ml of aqueous HCl at pH 1.5. The resultant solution was stirred for 20 h at 40 ºC, followed by aging at 110 ºC for 24 h under static conditions. The solid product was recovered by filtration, dried at room temperature overnight and calcined at 500 ºC for 5 h (heating rate = 0.4 ºC min^{-1}). **The supports so synthesized were called AlSBA(n) being "n" the Si/Al ratio of the calcined solid determined by ICP analysis.**

Chromium grafting procedure started with calcined support materials outgassed under vacuum conditions overnight. Then, samples were stirred with 250 ml of chromium (III) acetylacetonate ($Cr(acac)_3$) solution in toluene for 2 hours under reflux. Next, solids were

recovered by filtration and intensively washed with toluene. Finally, grafted materials were calcined with air on a fluidized bed reactor up to 600 ºC for 3 h with a heating rate of 1.8 ºC min^{-1}. **The obtained catalysts were denoted as Cr-support name-x being "x" the chromium content (wt %) determined by ICP analysis.**

2.2. Catalysts characterization.

Nitrogen adsorption-desorption isotherms at 77 K were obtained with a Micromeritics Tristar 3000 apparatus. The samples were previously out-gassed under vacuum at 250 ºC for 4 hours. Surface areas were calculated with BET equation whereas pore size distributions were determined by the BJH method applied to the adsorption branch of the isotherms. Mean pore size was obtained from the maximum of BJH pore size distribution. X-ray powder diffraction (XRD) data were acquired on a Philips X'PERT MPD diffractometer using Cu Kα radiation. Solid state NMR of ^{27}Al nuclei spectra were obtained on a Varian 400 MHz spectrometer with the following conditions: magic-angle spinning at 6 kHz; π/2 pulse = 3 μs; repetition delay = 2 s. The NMR of ^{27}Al spectra were referenced to hydrated $AlCl_3$. Transmission electron microscopy measurements were performed on a 200 kV Philips Tecnai 20 electron microscope.

Fourier transform IR (FT-IR) spectra of fresh catalysts were recorded on a Mattson Infinity Series spectrophotometer using the potassium bromide wafer technique. Diffuse reflectance UV-VIS spectra (DRS) of the as-synthesized and calcined chromium mesoporous materials were obtained under ambient conditions on a CARY-1 spectrophotometer equipped with a diffuse reflectance accessory in the wavelength range of 300-700 nm. A halon white reflectance standard was used as a reference material. Thermogravimetric measurements (TGA) were performed in air flow on a TA instrument SDT 2960 thermobalance, with a heating rate of 5º C/min up to 700 ºC. Catalysts chemical composition was measured by ICP-atomic emission spectroscopy on a Varian Vista AX CD system. Hexavalent chromium species in calcined catalysts were analyzed by

temperature-programmed reduction (TPR) in a TPD/TPR Micromeritics AutoChem 2090 apparatus using a flow of Ar/H_2 (10 % of H_2) with a heating rate of 35 ºC min^{-1} from 100 to 600 ºC. A TC detector was used to determine the hydrogen consumption.

2.3. Polymerization tests and polymer characterization.

Ethylene polymerization reactions were carried out in a 2-litres stainless steel stirred Autoclave Engineers apparatus. Reaction conditions were 600 r.p.m., 85 ºC, 35 bar of ethylene, 5.0 bar of hydrogen, 0.5 mol of 1-hexene using isobutane as solvent. After one hour of reaction, the resulting polyethylene (PE) was recovered, filtered, washed with acetone and dried for 6 hours at 70ºC. Polymerization activities (Kg PE/g Cr h) were calculated dividing the weight of dry PE produced by the weight of chromium in the catalyst.

DSC analysis of the obtained polymers were recorded from 50 to 180 ºC (heating rate = 10 ºC min^{-1}) with a Mettler Toledo DSC822 apparatus. High load melt index (HLMI) values were determined at 190 ºC with a weight load of 21.6 kg using a Ceast 6542/002 extrusion plastometer. The polyethylene bulk density was determined from the dry weight and the volume of the sample in a volumetric tube by liquid displacement. Polymers mean molecular weight and molecular weight distributions were determined by size-exclusion chromatography at 145°C on a Waters 150C Plus instrument, using 1,2,4-trichlorobencene as mobile phase. The column set consisted of one PL-Gel 10μm Mixed B (300 x 7.5 mm) and another Polymer PL-Gel 10 μm 10E6A (300 x 7.5 mm). The columns were calibrated with 11 polystyrene standards (narrow molar mass distribution in the range: 2960-2700000) and with one high polydispersity polyethylene standard (from NIST, Mw = 53070).

3. Results and discussion

3.1. Support Characterization.

X-ray diffraction patterns of the calcined mesoporous supports, denoted as SBA-15 and AlSBA(n) (n = Si/Al ratio), are illustrated in figure 1. All materials exhibit well resolved diffraction peaks that can be indexed as the (100), (110) and (200) reflections associated with p6mm hexagonal symmetry typical of SBA-15 materials [12, 15]. **These peaks are slightly shifted to lower angle values when increasing aluminium content indicating a higher d-spacing. This fact can be a consequence of the longer Al-O bond length compared to the Si-O bond [ref1, ref2], so that, the aluminium incorporation produces a slight swelling effect on the solid structure.**

Nitrogen adsorption-desorption isotherms, presented in figure 2, show a clear H1-type hysteresis loop at high relative pressure values, typical for SBA-15 mesoporous materials [12, 15]. Table 1 summarizes the textural properties of the SBA-15 supports. It can be observed that BET surface area, pore size and pore volume increase upon insertion of aluminium in agreement with the literature [16, 17]. Besides, larger pores detected in AlSBA materials are responsible of the lower wall thickness values as shown in table 1. It is remarkable that important changes in the textural properties are produced when a low amount of aluminium is incorporated into SBA-15 material. However, not meaningful differences in these textural properties were detected changing the Si/Al ratio of the materials. Table 1 also displays the textural properties of a Crosfield commercial silica used as a reference support to prepare Cr-SiO_2 catalysts, for comparison purposes.

Table 1 also shows an important reduction in the aluminium incorporation from the synthesis gel to the mesostrutured solids when decreasing the initial content of aluminium. Thus, aluminium incorporation degree is 100 % in AlSBA(30) sample, 70 % in AlSBA(86) and 58 % in AlSBA(156).This phenomenon is probably related to the synthesis procedure of

AlSBA materials [15, 16], which depends on the mixture acidity. Thus, at pH = 1.5, aluminium is highly incorporated to the SBA-15 structure if the Si/Al ratio keeps lower than 30. In fact, Yue et al. [15, 16] prepared AlSBA-15 samples with Si/Al ratio around 10 and 20. Presumably, a decrease of the aluminium concentration in the synthesis mixture makes difficult the interaction between Al atoms to form Al_2O_3 species (hexa-coordinated centres) and the incorporation of aluminium in the framework (four-coordinated centres) is the principal mechanism to keep the concentration from the initial solution to the final solid. Moreover, according to the literature, using direct-synthesis methods in a acid medium, only a part of the aluminium atoms added in the initial gel can be introduced into the mesostructure from aqueous solution [14]. So that, working with lower Si/Al ratio it is possible to obtain higher aluminium incorporation degree although the ratio of tetrahedral to octahedral aluminium trends to decrease. This explanation are confirmed by ^{27}Al MAS NMR spectra of AlSBA-15 samples, presented in the figure 3. It can be seen that aluminium was mainly incorporated with tetrahedral coordination in the SBA-15 framework, as evidenced by the main signal at δ = 54 ppm and the less intense signal at δ = 0 ppm, corresponding to octahedral aluminium. As well the decrease of the [Al tetrahedral]/[Al octahedral] ratio with the growth of the aluminium content is observed (see table 1).

Finally**,** transmission electron microscopy images (figure 4) show well ordered hexagonal arrays of 1D mesoporous channels and confirm that the AlSBA samples have a 2D P6mm hexagonal structure, representative of SBA-15 materials. The pore sizes estimated from the TEM images are around 110-120 Å (very similar to values determined by BJH method from N_2 adsorption isotherms).

3.2. Chromium incorporation and catalyst characterization.

Table 2 lists the grafting efficiencies achieved in the preparation of Cr-SBA and Cr-AlSBA catalysts using a starting solution of chromium (III) acetilacetonate, $Cr(acac)_3$, in toluene with 5 wt % of chromium. According to previous investigations, **the amount of chromium anchored onto Al-MCM-41 materials increases with aluminium incorporation** to the supports [18]. Grafting experiments with AlSBA-15 materials, carried out in the present work, show the same tendency.

In this way, the grafting over siliceous SBA-15, AlSBA(156), AlSBA(86) and silica produces catalysts having a low chromium content for ethylene polymerization. In order to obtain catalysts with a higher chromium content (approximately 1 wt %, which is the usual value for ethylene polymerization in slurry phase), it was necessary to increase the chromium concentration of the starting grafting solution from 5 wt % up to 56 wt %. So, three samples were prepared and called Cr-AlSBA(156)-0.97, Cr-SBA-0.93 and Cr-SiO_2-0.90 being their chromium content 0.97, 0.93 and 0.90 wt % respectively (see table 2).

The increase in grafting efficiencies with the aluminium content may be related to the different interactions established between the $Cr(acac)_3$ complex and silicon or aluminium surface atoms of the supports. DR UV-Vis spectroscopy, FTIR spectroscopy and TG analysis were used to study the nature of chromium species anchored to SBA-15 and AlSBA-15 materials.

Figure 5 (I) shows UV-Vis spectra of fresh Cr/SBA-15 catalysts and bulk $Cr(acac)_3$. Samples containing aluminium (Cr-AlSBA(156)-0.97; Cr-AlSBA(30)-0.90) and chromium acetilacetonate complex present the same colour (violet) and similar spectra with typical Cr (III) d-d absorption bands centred at 325, 390 and 560 nm, which can be attributed to $^4A_{2g} \rightarrow {}^4T_{2g}$ (F), $^4A_{2g} \rightarrow {}^4T_{1g}$(F) and $^4A_{2g} \rightarrow {}^4T_{2g}$(P) transitions in the pseudo-octahedral coordinated chromium (III) ions, respectively [19]. Nevertheless, Cr-SBA-0.93 catalyst prepared using the SBA-15 siliceous support presents a greenish colour and the band placed at 390 nm has almost disappeared from the DR UV-Vis spectra. These facts indicate a change in the electron configuration of

chromium when a solution of $Cr(acac)_3$ complex in toluene reacts with silicon atoms from SBA-15 surface [20, 21].

Calcination of the as-synthesized samples resulted in the complete disappearance of these d-d bands (Figure 5 II) owing to Cr (III) oxidation to Cr(VI) ions. **The later, were characterized by three absorption bands at 240, 355 and 428 nm**, which can be assigned to the $O \rightarrow Cr^{6+}$ charge transfer transitions of chromate and dichromate [6, 22]. The absence of chromium (III) oxide band at 560 nm indicates the total oxidation of Cr^{3+} to Cr^{6+} during the calcination step in air stream.

The UV-Vis spectra of the calcined catalysts were deconvolutioned and the peak areas were calculated to know the ratio between the different $O \rightarrow Cr^{6+}$ signals. Figure 5 III shows the ratios obtained which indicate that the bands placed at lower wave length (245 and 355 nm), usually related to chromate species, increase with the presence of aluminium in the supports. As well, the signal located at 428 nm, corresponding to dichromate, decreases with the aluminium content. Therefore, high aluminium content promotes chromate species whereas siliceous solids involves a growth of polychromate groups. This tendency is in agreement with the results existing in the literature about characterization of conventional Phillips catalysts [6, 22].

FTIR spectra of SBA-15 and AlSBA(30) supports, $Cr(acac)_3$ bulk and chromium supported catalysts are showed in figure 6a and 6b. This technique allows to discriminate between chromium (III) acetylacetonate and aluminium acetylacetonate surface species basing on the fact that vibrations of carbon-oxygen and carbon-carbon bonds in acetylacetonate ligands coordinated to chromium and aluminium differ [21, 23], see table 3. **All the catalysts show the typical chromium acetylacetonate bands due to the vibration of the C=C bonds (1526 cm^{-1}), C-H bonds (1425 cm^{-1}) and C=O bonds (around 1374 and 1569 cm^{-1}) [23, 24]. However, the**

signals location of this last functional group is slightly distinct depending on the support composition. So, Cr-AlSBA(156)-0.97 and AlSBA(30)-0.90 present two peaks centred at 1371 and 1564 cm^{-1} corresponding to C=O vibration (figure 6b) whereas Cr-SBA-0.93 sample shows these signals situated at 1376 and 1571 cm^{-1} respectively. These differences could indicate that different chemical environment are generated during grafting procedure around C=O groups. Anyway, the three FTIR spectra suggest that acetylacetonate ligands retained their ring structure during the interaction with silica, SBA-15 and AlSBA-15 supports and no aluminium acetylacetonate species were found on Cr-AlSBA catalysts after grafting with chromium (III) acetylacetonate under our experimental conditions.

The removal of the acetylacetonate ligands from the chromium complexes grafted onto the surface of SBA-15 and AlSBA-15 materials was studied by thermogravimetric analysis, as shown in figure 7. Cr-AlSBA catalysts presented the same TG profile as Cr-AlSBA(30)-0.90 and were not included in figure 7 for simplicity. The chromium loading and the observed weight loss of each sample associated with the removal of the acetylacetonate ligands, allow the calculation of the (acetylacetonate/Cr) ratio in the chromium surface species. The number of acetylacetonate molecules per chromium atom was found to be 3 in all samples. Considering these (acetylacetonate/Cr) ratios and the results obtained by UV-Vis and FTIR spectroscopy, it is possible to propose two different interaction mechanisms between the different supports and the chromium (III) acetylacetonate molecules:

1. During the grafting procedure using AlSBA-15, H-bonding between acetylacetonate ligands and hydroxyl groups of the mesoporous materials can be established (figure 8) [25, **26**]. It can be seen that supported chromium species present the same electronic environment as bulk $Cr(acac)_3$. Besides, two kinds of acetylacetonate ligands are observed:

- Two acetylacetonate ligands hydrogen bonded with hydroxyl groups.

- One acetylacetonate ligand unfavourable oriented for the interaction with surface active sites.

Removal of acetylacetonate ligands forming hydrogen bonds with surface hydroxyl groups is assisted by proton transfer and occurs under mild conditions (TGA peak at 240 ºC), while the acetylacetonate ligand not involved in hydrogen bonding was removed at higher temperatures (TGA peak at 335 ºC) [20].

2. When siliceous SBA-15 is used as support, a ligand exchange reaction may occur leading to chromium species with a different electronic environment than in the metallic precursor (figure 9) [25]. The greenish colour observed in Cr-SBA-0.93 catalyst and the disappearance of the band centred at 390 nm in UV-Vis spectra, are in agreement with this proposed mechanism. In this case, the first weight loss in the TGA profile showed in figure 7 (peak at 250 ºC), could be related to the elimination of acetylacetonate ligands retained over the siliceous supports after the ligand exchange reaction. The second weight loss (peak at 320 ºC) could be produced by the decomposition of remaining acetylacetonate ligands (acac groups attached on chromium centres).

The H_2-TPR profiles of activated catalysts along with the individual peaks obtained by means of computer deconvolution are showed in the figure 10. It can be observed that Cr/SBA-15 catalysts show a single signal which suggests a single reduction step of hexavalent to trivalent chromium species due to the reaction with the H_2 molecules [26-30]. Deconvolution of TPR signals of Cr-SBA-0.93, Cr-AlSBA(156)-0.97 and Cr-AlSBA(30)-0.90 catalysts displays two peaks indicating the presence of two types of Cr(VI) centres, **the temperature and the H_2 consumption associated to each peak of these TPR analysis are summarized in the table 4** . High temperature peak (375 – 398 ºC) could be assigned to chromates reduction while low TPR peak (334- 347 ºC) may be related with the hydrolysis of Si-O-Cr and Al-O-Cr bonds to produce CrO_3. Chromium (VI) oxide species are mobile and, therefore, can agglomerate to form large

chromium species, which can be reduced by the hydrogen at lower temperatures [28]. It is noticeable how chromium reduction temperatures decrease with Si/Al ratio of AlSBA-15 support. However, TPR data for Cr-SBA-0.93 are not comparable since siliceous SBA-15 support has much lower surface area and pore size than the AlSBA-15 supports (see table 1).

3.3. Ethylene polymerization results

Table 5 presents the ethylene polymerization activities of Cr/SBA-15 catalysts compared to the conventional Cr/SiO_2 catalyst prepared from the commercial silica (table 1) as well as the main properties of the resulting polymers: molecular weight, polydispersity index, melt temperature, High Load Melt Index (HLMI) and bulk density.

It is remarkable the very low catalytic activity showed by Cr-SBA-0.93 sample, in spite of the high surface area of SBA-15, usually related to high activities. The probable explanation is that the polymer just formed immediately fills up the pores of the material and, at the same time, since the catalyst structure is not fragile enough, it does not fragment into smaller pieces. So that the material can not produce further polymer and no subsequent activity is observed. Fragility is often correlated with pore volume. Thus, Cr/silica catalysts containing much less than 1.0 cm^3/g pore volume and 100 Å pore size, usually do not exhibit polymerization activity [2, 31]. In this way, small pore size, small pore volume and high wall thickness of SBA-15 support (see table 1) are responsible for the low polymerization activity exhibited by Cr-SBA-0.93 catalyst. So, it would be necessary to increase both pore size and pore volume of siliceous SBA-15 mesoporous material to get a suitable support to prepare Phillips type catalysts useful for ethylene polymerization. A possible way to do it is to use a swelling agent during the synthesis step. This approach has been already explored in a previous work of our group [32] using trimethylbenzene in the synthesis of siliceous SBA-15 mesoporous materials to prepare a Cr/SBA-15 catalysts with better catalytic activities than conventional Cr/SiO_2.

In this paper the effect of aluminium incorporation has been evaluated, as explained below. Table 5 shows that both Cr-AlSBA(156)-0.97 and Cr-AlSBA(30)-0.90 catalysts display a high catalytic activity. It can be observed that Cr-AlSBA(156)-0.97 sample produces about twice polyethylene than the Cr-SiO_2-0.90 catalyst and Cr-AlSBA(30)-0.90 sample, the richest in aluminium, is almost four times more active than Cr-SiO_2-0.90 catalyst. Therefore, it is clear that the polymerization activities of Cr/AlSBA-15 catalysts are significantly improved by increasing aluminium content of the AlSBA-15 supports. This fact could be explained taking into account that wall thickness of AlSBA-15 samples are reduced by decreasing the Si/Al ratio, resulting at the same time in higher pore volumes (see table 1). These two circumstances lead to more fragile materials and consequently more active in ethylene polymerization. Besides, hydrogen TPR analysis indicated that hexavalent chromium species grafted onto AlSBA(30) are more easily reducible (Tmax = 369 ºC) than those deposited onto AlSBA(156) (Tmax = 379 ºC).

Regarding polymer properties, all catalysts produced high density polyethylene with melting temperatures around 131 ºC. The polymer molecular weight (MW) obtained also depends on the catalyst porosity and, according to McDaniel [2], larger pore diameters seem to yield lower MW. In this sense, polyethylene produced with AlSBA-15 catalysts had almost the same molecular weight. However, polyethylene obtained with the conventional catalyst (Cr-SiO_2-0.90) presented lower MW because of the higher pore size of the silica support (see table 1). As a consequence, the polymer obtained with the conventional Cr/SiO_2 catalyst showed higher melt index (HLMI) than polyethylene obtained using Cr/AlSBA-15 catalysts. The different proportion of long chain branching in polyethylene structure of the products obtained with Cr-AlSBA(30)-0.90 and Cr-AlSBA(156)-0.97 catalysts could explain the changes observed in High Load Melt Index (HLMI) and polydispersity index values [33].

4. Conclusions

Ethylene polymerization catalysts have been prepared by grafting chromium (III) acetylacetonate onto SBA-15 (Si/Al = ∞, 156, 86 and 30) mesoporous materials. BET surface area, pore size and pore volume of SBA-15 supports increase upon insertion of aluminium, while lower wall thickness values are obtained.

Aluminium incorporation favours chromium anchorage onto SBA-15 surface. According to IR and UV-Vis spectra of fresh catalysts, the ligands of the supported complex retain their ring structure and no aluminium-acetylacetonate species are found when chromium (III) acetylacetonate is grafted onto AlSBA-15 samples under our experimental conditions.

Uncalcined Cr/AlSBA-15 samples show the same colour (violet) and UV-vis spectrum than the bulk $Cr(acac)_3$. Nevertheless, fresh siliceous SBA-15 sample shows a greenish colour. Calcination of the as-synthesized catalysts results in the complete oxidation of Cr(III) to Cr(VI). The latter was characterized by two adsorption bands at 350 and 460 nm assigned to the $O \rightarrow Cr^{6+}$ charge transfer transitions of chromate and dichromate, whose reduction temperature (determined by hydrogen TPR) decreases with the Si/Al ratio of the AlSBA-15 supports.

The interaction of chromium acetylacetonate molecules with SBA-15 supports occurs without a loss of acac ligands, since the (acac/Cr) ratios found in the chromium complexes fixed to SBA-15 and AlSBA-15 surface are around three in all the prepared catalysts. The attachment of Cr species to AlSBA-15 surface results from interaction of hydroxyls groups with the acetylacetonate ligands through H-bonds, while a ligand exchange reaction might occur over siliceous SBA-15.

Small pore size (80 Å), pore volume (0.96 cc/g) and high wall thickness (38 Å) of siliceous SBA-15 support are responsible of lower polymerization activity exhibited by the Cr/SBA-15 catalyst. On the contrary, Cr/AlSBA-15 samples show high polymerization activity values. Particularly, catalyst prepared with the AlSBA-15 (Si/Al = 30) support is almost four times more active than a conventional Cr/SiO_2 Phillips catalyst. The behaviour of Cr/AlSBA-15 samples may be connected with their low wall thickness values (between 14 and 11 Å) which lead to more fragile materials and, therefore, more active catalysts.

Regarding polymer properties, all catalysts produce high density polyethylene with similar molecular weights and melting temperatures around 131 ºC. Only, Cr/SiO_2 catalyst gives PE with lower molecular weight because of the wider pores of silica compared to mesostructured SBA-15 material.

Consequently, AlSBA-15 supports could be an attractive alternative to replace conventional amorphous supports like silica and alumina in the Phillips polymerization process.

References

[1] J. P. Hogan, R. L. Banks, US Patent 2, 825, 721, (1958), to Phillips Petroleum Corporation.

[2] M. P. McDaniel, Adv. Catal. 33 (1985) 47.

[3] B. M. Weckhuysen, R. A. Schoonheydt, Catal. Today. 51 (1999) 215.

[4] S. L. Scott, J. Amor Nait Ajjou, Chem. Eng. Sci. 56 (2001) 4155.

[5] G. Ertl, H. Knozinger, J. Weitkamp (Ed.), Handbook of Heterogeneous Catalysis, VCH. Verlagschaft, vol. 5, 1997, p. 2400.

[6] B. M. Weckhuysen, I. E. Wachs, R. A. Schoonheydt, Chem. Rev. 96 (1996) 3327.

[7] T. J. Pullukat, R. E. Hoff, M. J. Shida, Polym. Sci. Polym. Chem. Ed. 18 (1980) 2857.

[8] S. J. Conway, J.W. Falconer, C. H. Rochester, J. Chem. Soc. Faraday Trans I. 85 (1989) 71.

[9] M. P. McDaniel, D. R. Uit, E. A. Benham, J. Catal. 176 (1998) 344.

[10] R. Ramachandra , B. M. Weckhuysen, R. A. Schoonheydt, Chem. Commun. (1999) 445.

[11] B. M. Weckhuysen, R. Ramachandra, J. Pelgrims, R. A. Schoonheydt, P. Bodart, G. Debras, O. Collart, P. Van Der Voort, E. F. Vansant, Chem. Eur. J. 6 (2000) 2960.

[12] D. Zhao, J. Feng, Q. Huo, N. Melosh, G. H. Fredrickson, B. F. Chmelka, G. D. Stucky, Science. 279 (1998) 548.

[13] D. Zhao, Q. Huo, J. Feng, B. F. Chmelka, G. D. Stucky, J. Am. Chem. Soc. 120 (1998) 6024.

[14] S. Wu, Y. Han, Y.-C. Zou, J.-W. Song, L. Zhao, Y. Di, S.-Z. Liu, F.-S. Xiao, Chem. Mater. 16 (2004) 486.

[15] Y. Yue, A. Gédéon, J.-L. Bonardet, N. Melosh, J.-B. D'Espinose, J. Fraissard, Chem. Comm. (1999) 1967.

[16] Y.-H. Yue, A. Gédéon, J.-L. Bonardet, J. B. d'Espinose, N. Melosh, J. Fraissard, Stud. Surf. Sci. Catal. 129 (2000) 209.

[17] M.-A. Springuel-Huet, J.-L. Bonardet, A. Gédéon, Y. Yue, V.N. Romannikov, J. Fraissard, Micropor. Mesopor. Mater. 44–45 (2001) 775.

[18] G. Calleja, J. Aguado, A. Carrero, J. Moreno, Catal. Comm. 6(2) (2005) 153.

[19] A. B. P. Lever, Inorganic Electronic Spectroscopy, 2nd ed., Elsevier, Amsterdam, 1984.

[20] S. Haukka, E.-L. Lakomaa, T. Suntola, Appl. Surf. Sci. 75 (1994) 220.

[21] I. V. Babich, Y. V. Plyuto, P. Van der Voort, E. F. Vansant, J. Chem. Soc. Faraday Trans. 93 (1997) 3191.

[22] B. M. Weckhuysen , L. M. De Ridder, R. A. Schoonheydt, J. Phys. Chem. 97 (1993) 4756.

[23] Sh. M. Alexander, D. M. Bibby, R. F. Howe, R. H. Meinhold, Zeolites. 13 (1993) 441.

[24] L. Puurunen, S. M. K. Airaksinen, A. O .I. Krause, J. Catal. 213 (2003) 28

[25] I. V. Babich, Y. V. Plyuto, P. Van der Voort, E. F. Vansant, J. Colloid. Interf. Sci. 189 (1997) 144.

[26] A. Ellison, T. L. Overton, L. Bencze, J. Chem. Soc. Faraday Trans. 89 (1993) 843.

[27] A. B. Gaspar, J. L. F. Brito, L. C. Dieguez, J. Mol. Catal. A: Chem. 203 (2003) 251.

[28] C. S. Kim, S. I. Woo, J. Mol. Catal. 73 (1992) 249.

[29] J. Santamaría-González, J. Mérida-Robles, M. Alcántara-Rodríguez, P. Maireles-Torres, E. Rodríguez-Castellón, A. Jiménez-López, Catal. Lett. 64 (2000) 209.

[30] M. Cherian, M. S. Rao, A. M. Hirt, I. E. Wachs, G. Deo, J. Catal. 211 (2002) 482.

[31] M. P. McDaniel, D. R. Witt, and E. A. Benham, J. Catal. 176 (1998) 344.

[32] G. Calleja, J. Aguado, A. Carrero, J. Moreno, Stud. Surf. Sci. Catal. 158 B (2005) 1453.

[33] M. P. McDaniel, D. C. Rohlfing, E. A. Benham, Polym. React. Eng. 11 (2003) 101.

TABLE 1. Physicochemical properties of silica and SBA-15 supports.

Support	*Synthesis (Si/Al)*	*Final (Si/Al)*[a]	$\left[\frac{Al_{tetra}}{Al_{octa}}\right]^b$	*BET Surface Area (m^2/g)*	*Pore Volume (cm^3/g)*	*Pore Size (Å)*[c]	*Wall thickness (Å)*[d]
SBA-15	∞	∞	--	651	0.96	80	38
AlSBA(156)	90	156	2.8	835	1.28	119	14

AlSBA(86)	60	86	2.6	784	1.32	114	11
AlSBA(30)	30	30	1.9	788	1.34	120	11
SiO_2[e]		--	--	286	1.71	290	--

[a] Determined by ICP analysis

[b] Determined from ^{27}Al-NMR (area δ = 54 ppm / area δ = 0 ppm)

[c] Determined from the maximum of BJH pore size distribution

[d] Wall thickness were calculated as: a_0 - pore size (a_0=2 x d (100)/$\sqrt{3}$)

[e] Supplied by Crosfield

TABLE 2. Chromium content of prepared catalysts.

Catalyst	Grafting solution $\left(\frac{g\ Cr\ (\text{solution})}{g\ \text{support}}\right)$ x100	Cr loading (wt %)[a]	Cr incorporation degree (%)
Cr-SBA-0.33	5	0.33	6.6

Cr-AlSBA(156)-0.53	5	0.53	10.6
Cr-AlSBA(86)-0.59	5	0.59	11.8
Cr-AlSBA(30)-0.90	5	0.90	18.0
Cr-SiO_2-0.90	56	0.90	1.5
Cr-SBA-0.93	56	0.93	1.7
Cr-AlSBA(156)-0.97	10	0.97	9.7

[a] Determined by ICP analysis

TABLE 3. IR bands (cm^{-1}) observed in FTIR spectra of bulk $Cr(acac)_3$ and $Al(acac)_3$, [21].

Bulk $Cr(acac)_3$	Bulk $Al(acac)_3$	Assignment
1575	1592	$\nu(C=O)_s$
1522	1533	$\nu(C=C=C)_{as}$
1426	1467	$\nu(CH_3)$

1383	1400	$\nu(C=O)_{as}$

TABLE 4. H_2 consumption and signals temperature obtained by deconvolution of TPR results.

Catalysts	1st Signal		2nd Signal	
	T(ºC)	H_2 consumed	T(ºC)	H_2 consumed

		(mmol/g)		(mmol/g)
Cr-SBA-0.93	344	0.106	393	0.156
Cr-AlSBA(156)-0.97	347	0.135	390	0.140
Cr-AlSBA(30)-0.90	295	0.060	368	0.196

TABLE 5. Ethylene polymerization results with silica and SBA-15 chromium supported catalysts.

(T = 90 ºC; $P_{ethylene}$ = 35 bar; $P_{hydrogen}$ = 5.0 bar ; 0.5 mol of 1-hexene; Solvent = isobutane).

Catalyst	Activity (kg PE/g Cr h)	Mw	Mw/Mn	T_m (ºC)[a]	HLMI (g/10 min)	Bulk Density (g/ml)

Cr-SiO_2-0.90	146.9	300050	24.8	131.2	4.5	0.31
Cr-SBA-0.93	32.8	n.d	n.d	n.d	n.d	0.13
Cr-AlSBA(156)-0.97	224.9	373120	35.6	131.6	1.8	0.27
Cr-AlSBA(30)-0.90	551.2	378060	45.1	131.5	3.6	0.26

n.d : not determined due to the low activity observed

[a] Melting temperature measured by DSC

Figure Captions

Figure 1. X-ray diffraction patterns of the calcined SBA-15 and AlSBA-15 supports.

Figure 2. N_2 adsorption-desorption isotherms at 77 K (I) and pore size distributions (II) of the calcined SBA-15 and AlSBA-15 supports.

Figure 3. ^{27}Al RMN spectra of the calcined AlSBA-15 samples.

Figure 4. TEM micrographs of the calcined SBA-15 samples with different Si/Al ratios: (a) SBA-15, (b) AlSBA(156), (c) AlSBA(86) and (d) AlSBA(30).

Figure 5. UV-Vis spectra of fresh (I) and calcined (II) chromium-containing SBA-15 catalysts: (a) Cr-SBA-0.93, (b) Cr-AlSBA(156)-0.97, (c) Cr-AlSBA(30)-0.90, (d) $Cr(acac)_3$. **(III) Ratios between deconvolutioned areas of UV-Vis signals.**

Figure 6. (I) FTIR spectra of (a) SBA-15 , (b) AlSBA(30) and (c) $Cr(acac)_3$ bulk. (II) FTIR spectra of uncalcined catalysts (a) Cr-SBA-0.93, (b) Cr-AlSBA(156)-0.97, (c) Cr-AlSBA(30)-0.90.

Figure 7. TG analysis of chromium-containing SBA-15 catalysts.

Figure 8. Anchorage mechanism of $Cr(acac)_3$ over aluminium-containing SBA-15 materials.

Figure 9. Anchorage mechanism of $Cr(acac)_3$ over free aluminium materials.

Figure 10. H_2-TPR profiles of activated chromium-containing SBA-15 catalysts.

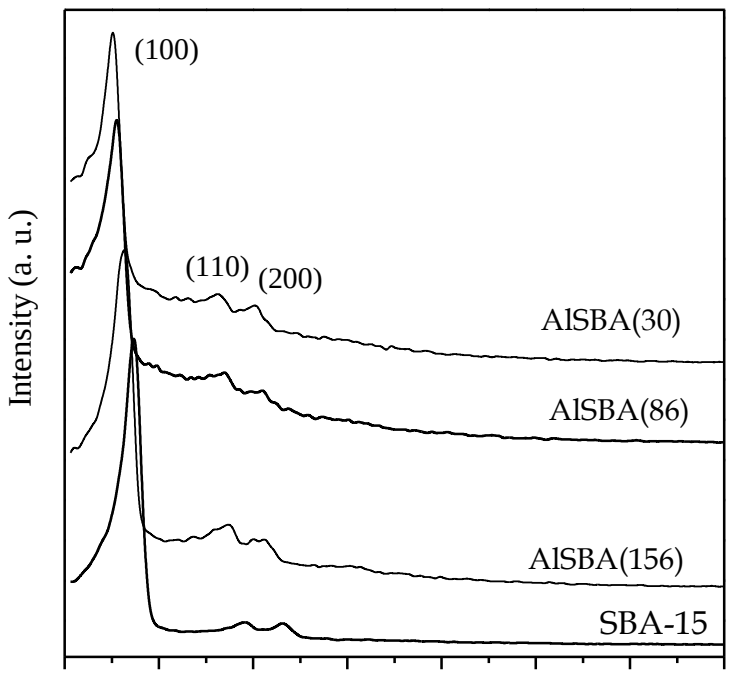

Figure 1

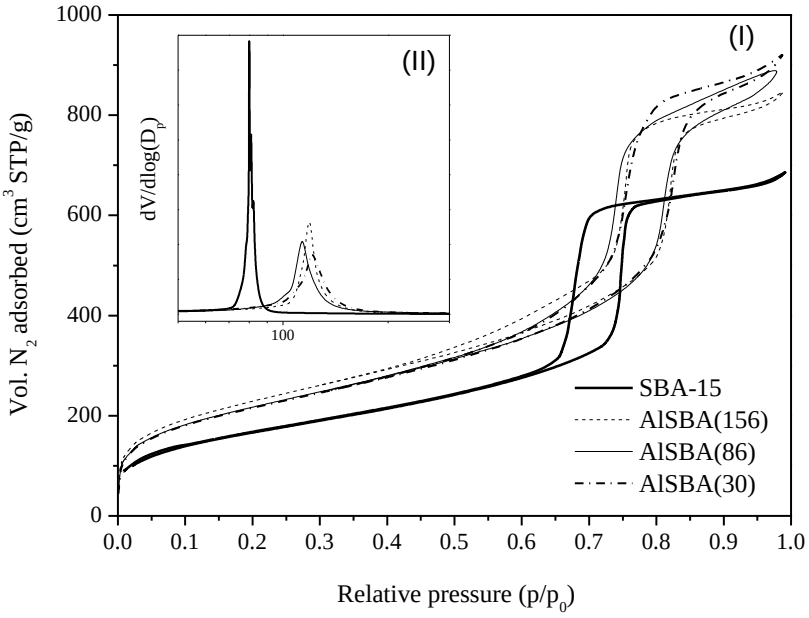

Figure 2

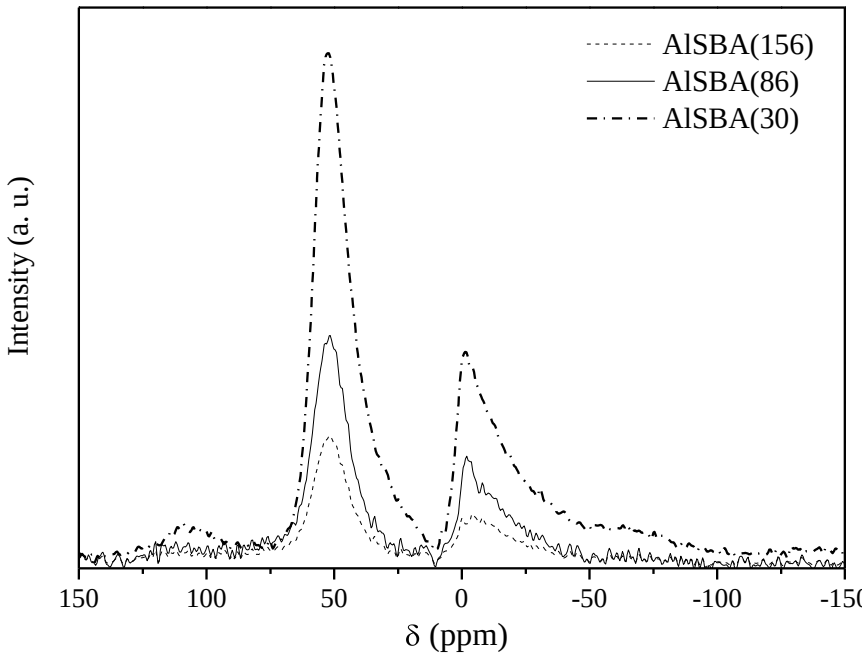
AlSBA(156)
AlSBA(86)
AlSBA(30)
Intensity (a. u.)
150
100
50
0
-50
-100
δ (ppm)

Figure 3

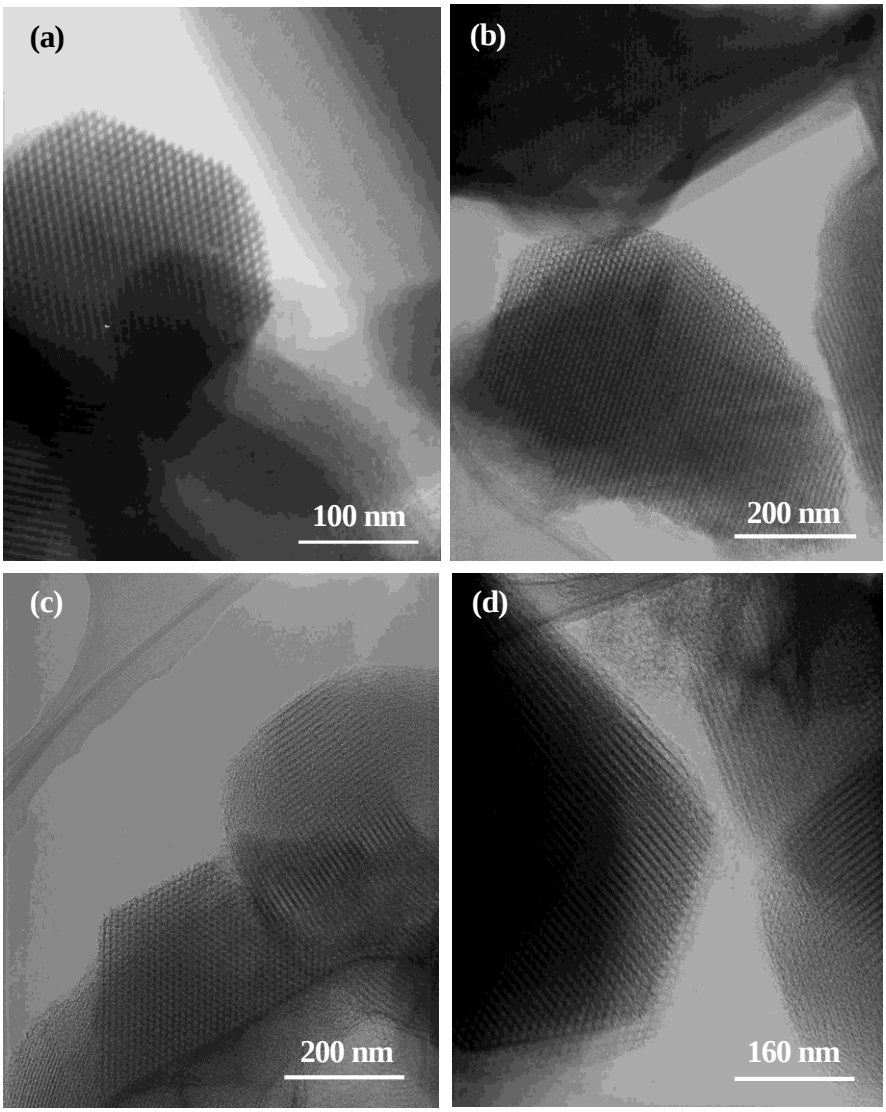

Figure 4

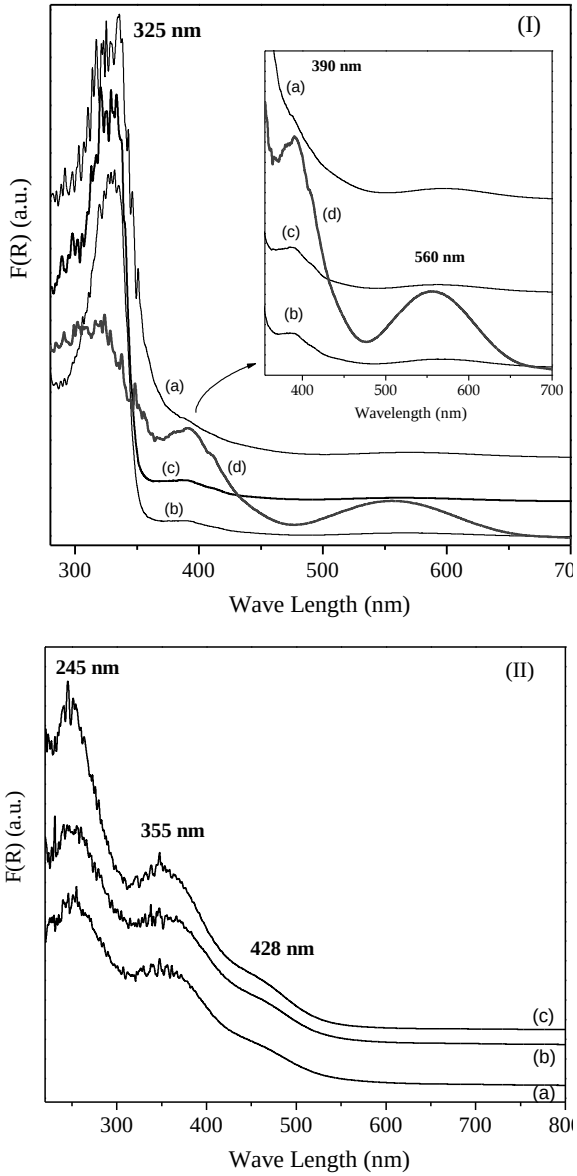
325 nm
(I)
390 nm
(a)
(d)
(c)
560 nm
(b)
400
500
600
700
Wavelength (nm)
F(R) (a.u.)
(a)
(c)
(d)
(b)
300
400
500
600
70
Wave Length (nm)
245 nm
(II)
355 nm
428 nm
(c)
(b)
(a)
F(R) (a.u.)
300
400
500
600
700
80
Wave Length (nm)

Figure 5

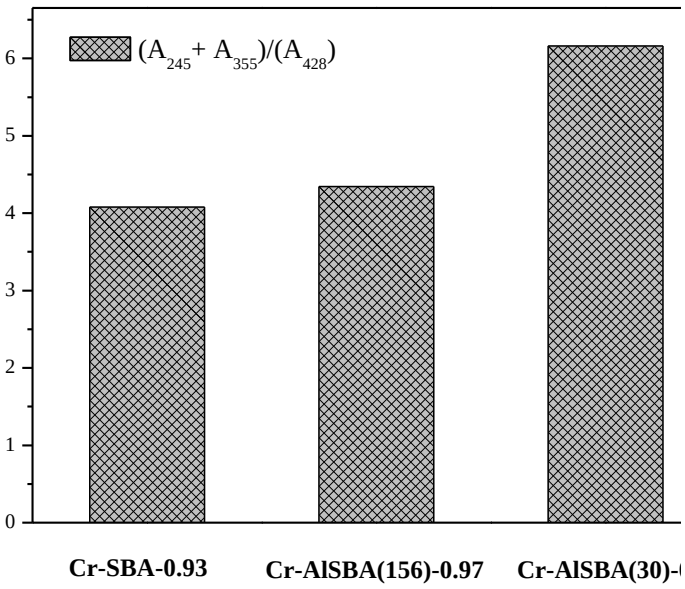

Figure 5

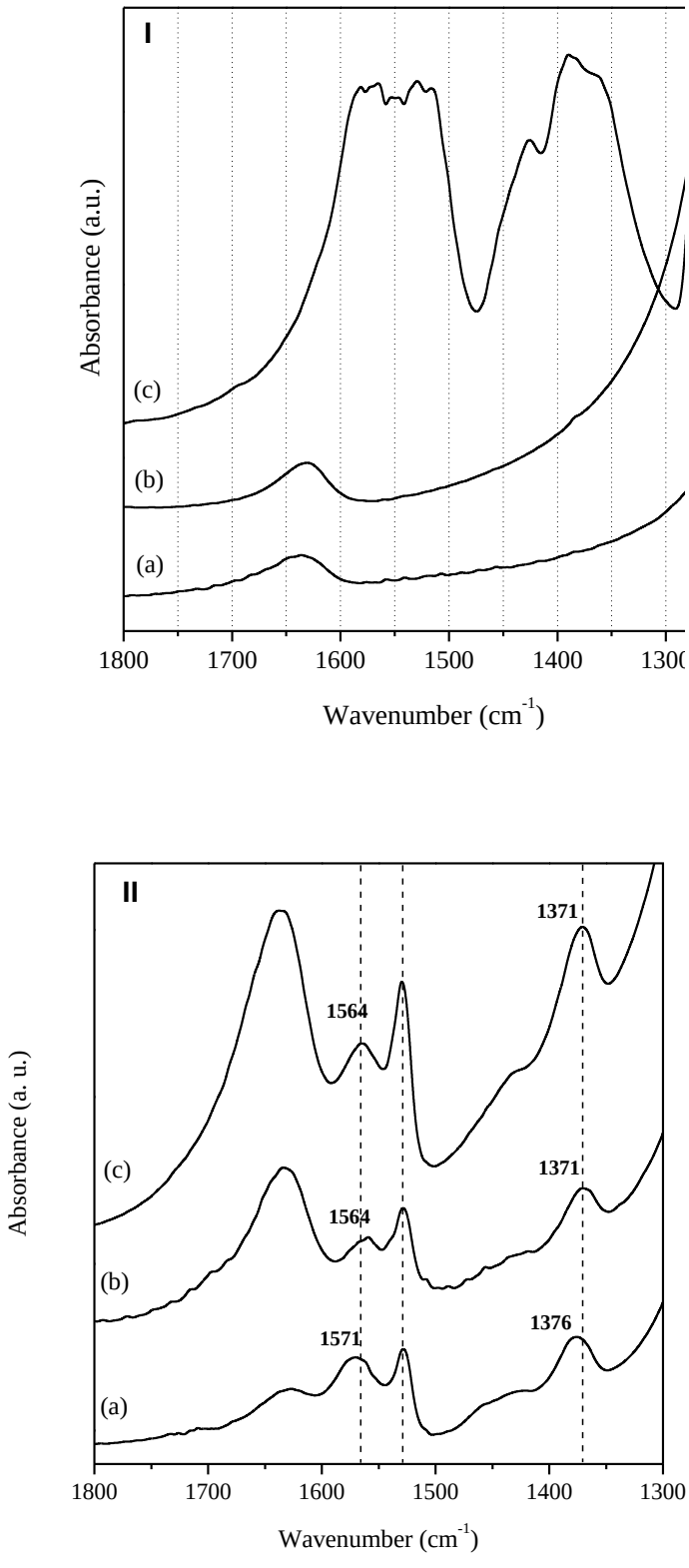
I
Absorbance (a.u.)
(c)
(b)
(a)
1800
1700
1600
1500
1400
1300
Wavenumber (cm-1)
II
1371
1564
(c)
1371
1564
(b)
1376
1571
(a)
Absorbance (a. u.)
1800
1700
1600
1500
1400
1300
Wavenumber (cm-1)

Figure 6

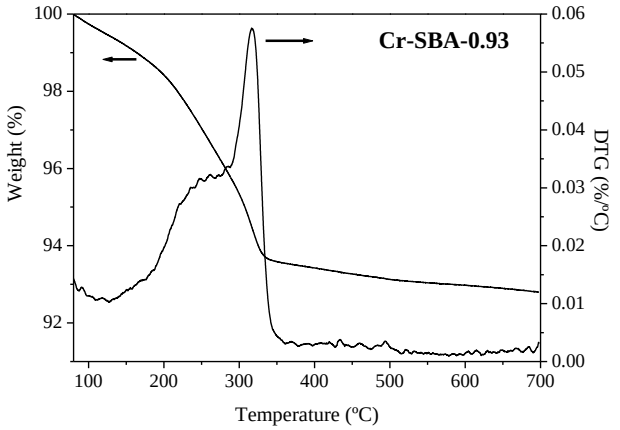
Cr-SBA-0.93
Weight (%)
DTG (%/ºC)
Temperature (ºC)
100
98
96
94
92
0.06
0.05
0.04
0.03
0.02
0.01
0.00
100
200
300
400
500
600
700

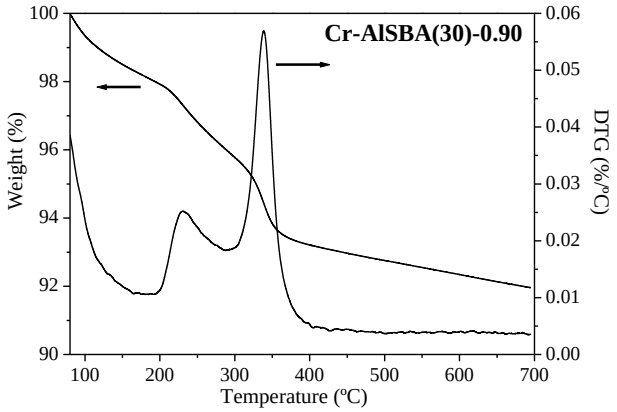
Cr-AlSBA(30)-0.90
Weight (%)
DTG (%/ºC)
Temperature (ºC)
100
98
96
94
92
90
0.06
0.05
0.04
0.03
0.02
0.01
0.00
100
200
300
400
500
600
700

Figure 7

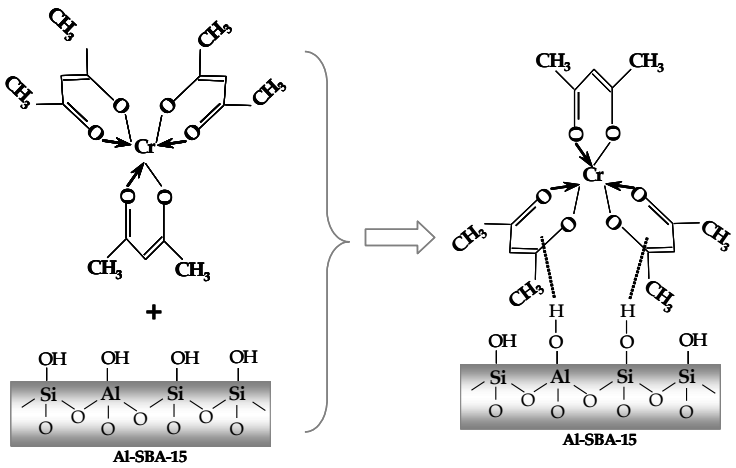

Figure 8

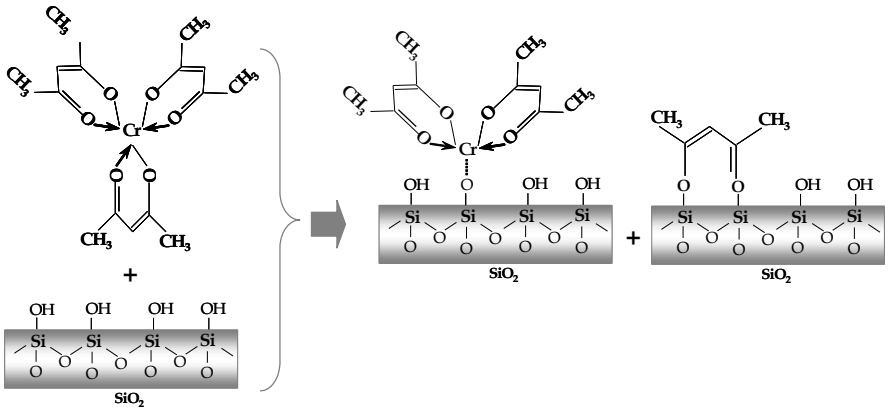

Figure 9

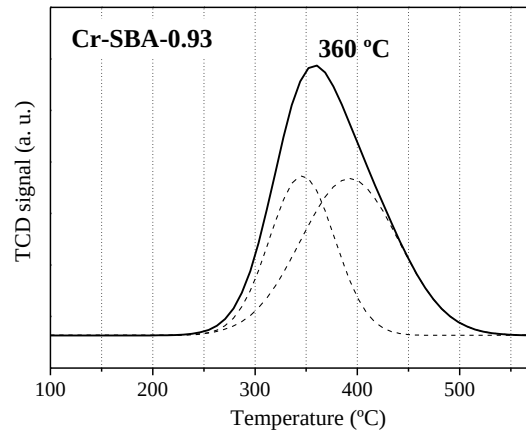
Cr-SBA-0.93
360 ºC
TCD signal (a. u.)
100
200
300
400
500
Temperature (ºC)

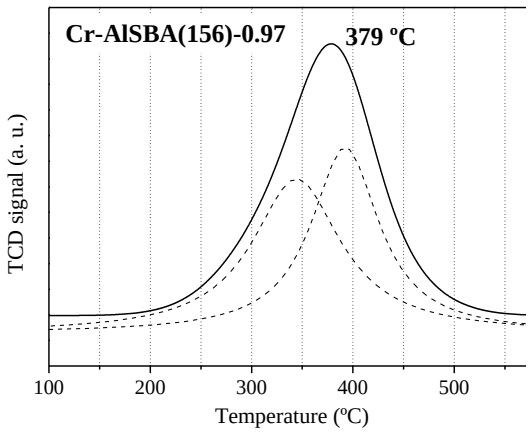
Cr-AlSBA(156)-0.97
379 ºC
TCD signal (a. u.)
100
200
300
400
500
Temperature (ºC)

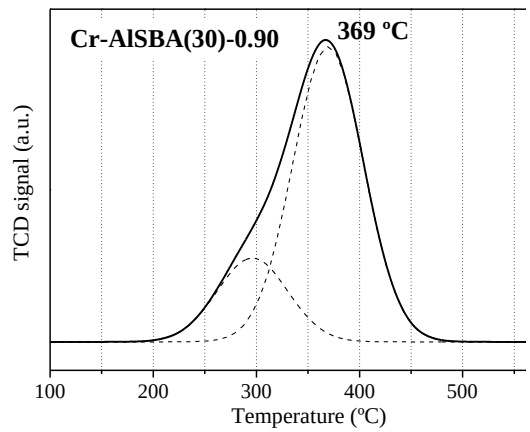
Cr-AlSBA(30)-0.90
369 ºC
TCD signal (a.u.)
100
200
300
400
500
Temperature (ºC)

Figure 10